

Erase then Rectify: A Training-Free Parameter Editing Approach for Cost-Effective Graph Unlearning

Zhe-Rui Yang^{1,2}, Jindong Han³, Chang-Dong Wang^{1,*}, Hao Liu^{2,3,*}

¹Sun Yat-sen University, Guangzhou, China

²The Hong Kong University of Science and Technology (Guangzhou), Guangzhou, China

³The Hong Kong University of Science and Technology, Hong Kong, China

yangzhr9@mail2.sysu.edu.cn, jhanao@connect.ust.hk, wangchd3@mail.sysu.edu.cn, liuh@ust.hk

*Corresponding author

Abstract

Graph unlearning, which aims to eliminate the influence of specific nodes, edges, or attributes from a trained Graph Neural Network (GNN), is essential in applications where privacy, bias, or data obsolescence is a concern. However, existing graph unlearning techniques often necessitate additional training on the remaining data, leading to significant computational costs, particularly with large-scale graphs. To address these challenges, we propose a two-stage training-free approach, *Erase then Rectify* (ETR), designed for efficient and scalable graph unlearning while preserving the model utility. Specifically, we first build a theoretical foundation showing that masking parameters critical for unlearned samples enables effective unlearning. Building on this insight, the Erase stage strategically edits model parameters to eliminate the impact of unlearned samples and their propagated influence on intercorrelated nodes. To further ensure the GNN's utility, the Rectify stage devises a gradient approximation method to estimate the model's gradient on the remaining dataset, which is then used to enhance model performance. Overall, ETR achieves graph unlearning without additional training or full training data access, significantly reducing computational overhead and preserving data privacy. Extensive experiments on seven public datasets demonstrate the consistent superiority of ETR in model utility, unlearning efficiency, and unlearning effectiveness, establishing it as a promising solution for real-world graph unlearning challenges.

Introduction

Machine unlearning has garnered considerable attention in recent years due to its ability to remove the influence of specific subsets of data from a well-trained machine learning model (Nguyen et al. 2022). This process is particularly important for forgetting sensitive, mislabeled, or obsoleted information. Typically, the subset of data to be unlearned is much smaller than the entire training dataset. As a result, one primary goal of machine unlearning is to efficiently eliminate the impact of these unlearned samples while preserving the model's predictive power, thereby avoiding the costly process of retraining the model from scratch on the remaining data (Xu et al. 2024).

In the graph domain, there is also a strong demand to forget specific information. For example, users in a social net-

work may request the removal of their personal data. In particular, Graph Neural Networks (GNNs) has become a common routine for processing and analyzing graph-structured data, leveraging message propagation and neighborhood aggregation mechanisms (Zhou et al. 2020). However, the interconnected nature of graphs determines that unlearned samples can significantly impact their neighbors through message propagation, making conventional machine unlearning methods unapplicable (Cheng et al. 2023). Consequently, graph unlearning has emerged as a specialized machine unlearning task with the goal of removing unlearned samples and mitigating their influence on other intercorrelated nodes (Said et al. 2023).

Recently, several approaches have been proposed to address the challenges of graph unlearning. For instance, GIF (Wu et al. 2023a) and CGU (Chien, Pan, and Milenkovic 2023) directly approximate the parameter changes induced by data removal and update the affected parameters. Such methods primarily focus on forgetting unlearned samples while overlooking the predictive capability on remaining data, which can significantly compromise model utility (Li et al. 2024). To resolve this problem, some recent studies (Li et al. 2024; Wang, Huai, and Wang 2023) have simultaneously considered both predictive and unlearning objectives when an unlearning request is received. However, they typically necessitate additional training on the remaining data, which leads to significant computational overhead, particularly with large graphs, even if only a small number of unlearned samples are involved. The substantial computational resources required constrain the efficiency and scalability of these methods, thereby limiting their practicality in real-world applications.

In this work, we focus on developing an efficient and scalable graph unlearning method that preserves the utility of GNNs. However, achieving this goal is non-trivial. First, the interconnected nature of graph data means that unlearned samples can significantly affect their neighbors through message propagation, making it challenging to efficiently remove both the unlearned samples and their influence on other nodes. Second, the remaining dataset after unlearning is typically much larger than the unlearned subset, which can lead to substantial computational overhead when accessing the remaining data. Balancing the need to maintain model utility with the demand for low computational

overhead presents another significant challenge.

To tackle the above challenges, we propose **Erase then Rectify (ETR)**, a training-free, two-stage approach for cost-effective graph unlearning. Specifically, we first establish a theoretical foundation demonstrating that masking parameters critical to unlearned samples enables effective graph unlearning. Building on this theory, in the Erase stage, we propose a neighborhood-aware parameter editing strategy to effectively eliminate the impact of unlearned samples and their cascading effects on the entire graph, while minimizing the impact on model utility. In the Rectify stage, we introduce a subgraph-based gradient approximation method to efficiently estimate the gradient of the unlearned model on the remaining data, which is then used to further enhance the model performance. Notably, ETR achieves graph unlearning without requiring explicit model training or access to the entire training dataset, which not only avoids substantial computational overhead but also ensures data privacy and security. Overall, the main contributions are as follows:

- We theoretically prove that masking parameters crucial for unlearned samples enable effective graph unlearning.
- We propose a training-free neighborhood-aware parameter editing method for graph unlearning that effectively forgets unlearned samples and their influence on inter-correlated samples.
- We propose a gradient approximation method to enhance GNN performance on the remaining graph without requiring access to the entire training dataset, thereby ensuring efficiency and scalability on large-scale graphs.
- Extensive experiments demonstrate the model utility, unlearning efficiency, and unlearning efficacy of ETR. Notably, ETR achieves an average of 4583.9x less time and 4.2x less memory usage than retraining from scratch.

Related work

Graph Unlearning Graph unlearning methods can be categorized into exact and approximate approaches, aiming to obtain an unlearned model that is exactly or approximately equivalent to retraining from scratch (Said et al. 2023). Current efforts primarily focus on approximate graph unlearning. For example, GraphEraser (Chen et al. 2022) and GUIDE (Wang, Huai, and Wang 2023) follow the SISA (Bourtole et al. 2021) paradigm, proposing graph partitioning algorithms to divide the training set into multiple shards, with a separate model trained for each shard. Besides, some approaches (Wu et al. 2023a,b; Chen et al. 2023; Chien, Pan, and Milenkovic 2023) leverage influence functions to approximate the impact of unlearning requests on model parameters. GNNDelate (Cheng et al. 2023) freezes model parameters while training additional parameters to achieve graph unlearning, and MEGU (Li et al. 2024) simultaneously trains the model’s prediction and unlearning objectives. Despite the effectiveness, these methods still face limitations when scaling to large graphs.

Training-Free Machine Unlearning

Several training-free methods have been proposed for efficient machine unlearning. For example, Fisher Forget-

ting (Golatkar, Achille, and Soatto 2020a) and NTK (Golatkar, Achille, and Soatto 2020b) are weight scrubbing methods that add noise to parameters informative for unlearned samples. However, Fisher Forgetting is computationally expensive and sacrifices the model’s predictive performance (Tarun et al. 2023), while NTK relies on additional models to achieve unlearning. The most relevant work to ours is SSD (Foster, Schoepf, and Brintrup 2024), which achieves unlearning by dampening parameters crucial for the unlearned dataset but not for the remaining dataset. Unlike SSD, we account for the impact of unlearned samples on other samples through message propagation. Additionally, we propose adaptively selecting hyperparameters, enhancing the method’s versatility across different datasets. Furthermore, we introduce the Rectify strategy to improve the model performance on the remaining dataset.

Preliminaries

Notations and Background

In this paper, we employ $\mathcal{G} = (\mathcal{V}, \mathcal{E}, \mathcal{X})$ to denote a graph comprising $|\mathcal{V}|$ nodes and $|\mathcal{E}|$ edges. Each node $\mathbf{v}_i \in \mathcal{V}$ has a d -dimensional feature vector $\mathbf{x}_i \in \mathcal{X}$. A major category of GNNs is message-passing neural networks (MPNNs) (Gilmer et al. 2017), including models such as GCN (Kipf and Welling 2017) and GAT (Velickovic et al. 2018). MPNNs follow the “propagate-transform” paradigm: in each layer of the network, they propagate and aggregate features from neighboring nodes, and then transform these aggregated features to update each node’s representation (Gilmer et al. 2017). Following previous works (Chen et al. 2022; Said et al. 2023), we focus on the task of node classification in this study. We denote the training dataset as D , the unlearned dataset as D_f , the remaining dataset as D_r (i.e., $D \setminus D_f$), and the k -hop neighborhood of D_f as D_k .

Fisher Information Matrix (FIM)

The FIM utilizes the second-order derivative of the loss function to quantify the sensitivity of each parameter, thereby providing a measure of its importance with respect to the input samples (Guo et al. 2020). Specifically, for a distribution $p(y|x, w)$, the FIM and its first-order derivative property (Kay 1993) are given as follows:

$$F_D = \mathbb{E}_{x,y} [-\nabla_w^2 \log p(y|x, w)] \quad (1)$$

$$= \mathbb{E}_{x,y} [\nabla_w \log p(y|x, w) \nabla_w \log p(y|x, w)^T] \quad (2)$$

Notably, obtaining the FIM is computationally expensive. A common approach is to use its diagonal $\text{diag}(F)$ (Kirkpatrick et al. 2017), which can be computed efficiently using the first-order derivative. The i -th element of the diagonal of the FIM calculated over the dataset D is denoted as $F_{D,ii}$, representing the importance of the i -th parameter with respect to the dataset D .

Problem Statement

Given a graph \mathcal{G} , the optimal GNN model $f_{\mathcal{G}}$ trained on \mathcal{G} , and a graph unlearning request $\Delta\mathcal{G} = (\Delta\mathcal{V}, \Delta\mathcal{E}, \Delta\mathcal{X})$,

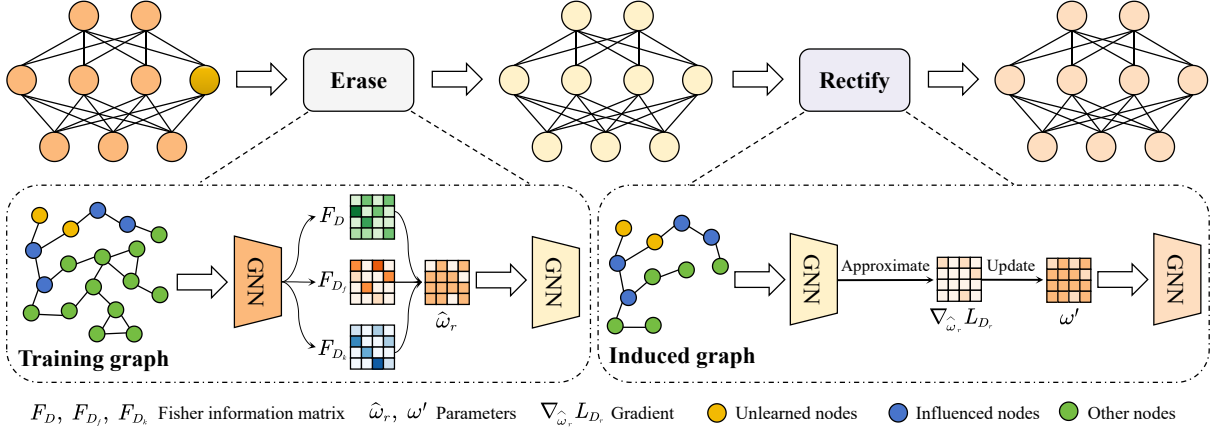


Figure 1: The framework of ETR: Forgetting the influence of unlearned samples through Erase, followed by enhancing the model performance on the remaining dataset via Rectify.

the objective of graph unlearning is to derive a new GNN model \hat{f} that minimizes the discrepancy between \hat{f} and $f_{\mathcal{G} \setminus \Delta \mathcal{G}}$. Here, $f_{\mathcal{G} \setminus \Delta \mathcal{G}}$ represents the GNN model retrained from scratch on the remaining graph $\mathcal{G} \setminus \Delta \mathcal{G}$.

Graph unlearning can be categorized into the following three tasks: **Node Unlearning:** $\Delta \mathcal{G} = (\Delta \mathcal{V}, \Delta \mathcal{E}, \Delta \mathcal{X})$, where $\Delta \mathcal{V}$ represents the unlearned nodes, $\Delta \mathcal{E}$ denotes the edges connecting to $\Delta \mathcal{V}$, and $\Delta \mathcal{X}$ represents the features of nodes in $\Delta \mathcal{V}$. **Edge Unlearning:** $\Delta \mathcal{G} = (\emptyset, \Delta \mathcal{E}, \emptyset)$, where $\Delta \mathcal{E}$ represents the set of edges to be unlearned. **Feature Unlearning:** $\Delta \mathcal{G} = (\emptyset, \emptyset, \Delta \mathcal{X})$, where $\Delta \mathcal{X}$ represents the unlearned features, and will be padded with zeros. We will use the node unlearning task to illustrate the proposed method, and describe how the proposed method applies to edge unlearning and feature unlearning tasks in the Appendix.

Methodology

Framework Overview

The overall framework of ETR is depicted in Figure 1. In the Erase stage, we evaluate parameter importance with respect to input samples based on the FIM. Subsequently, we identify critical parameters concerning the unlearned samples and their influence on other samples. We then modify these parameters to erase the effect of the unlearned samples. In the Rectify stage, we utilize the induced graph of unlearned samples to approximate model gradients on the remaining dataset, which are then used to enhance the model performance on the remaining dataset.

Graph Unlearning via Parameter Masking

Previous research indicates that certain neurons or parameters are critical in memorizing specific samples (Maini et al. 2023), and that gradient manipulation can prevent the memorization of noisy information (Chen et al. 2021). Motivated by these findings, we propose to achieve efficient unlearning by directly masking the parameters responsible for memorizing the data to be unlearned, as described below:

$$\hat{\omega}_{r,j} = \begin{cases} 0, & j \in M \\ \omega_j^*, & j \notin M \end{cases} \quad (3)$$

where ω^* represents the optimal parameters on D , and M denotes the set of parameters responsible for memorizing the unlearned dataset. To explore the effectiveness of the masking strategy, we provide theoretical justification for its ability to achieve graph unlearning as follows:

Theorem 1. *For a GNN model, if we approximate the FIM F with its diagonal $\text{diag}(F)$, and assume all elements of $\text{diag}(F)$ are strictly positive, the mean squared distance between the optimal model parameters trained on D_r and the parameters obtained from (3), denoted as $Q = \frac{1}{|\omega|} \sum_j (\omega_{r,j}^* - \hat{\omega}_{r,j})^2$, has the following upper bound:*

$$Q \leq \frac{1}{|\omega|} \left(c_1 \sum_{j \in M} \frac{1}{F_{D_r,jj}^2} + c_2 \sum_{j \notin M} \frac{F_{D_f,jj}^2}{F_{D,jj}^2 F_{D_r,jj}^2} + c_3 \right) \quad (4)$$

where c_1, c_2, c_3 are constants, and $|\omega|$ denotes the number of parameters.

The proof of Theorem 1 is provided in the Appendix. According to Theorem 1, adding the j -th parameter to M will increase the upper bound of Q by $\frac{1}{|\omega|} \left(\frac{c_1}{F_{D_r,jj}^2} - \frac{c_2 F_{D_f,jj}^2}{F_{D,jj}^2 F_{D_r,jj}^2} \right)$. This increase is less than 0 when $\frac{F_{D_f,jj}}{F_{D,jj}} > \sqrt{\frac{c_1}{c_2}} = c$, indicating that the parameter w_j is much more important for D_f than for D . Therefore, masking parameters that are crucial for unlearned samples but not for others can reduce the upper bound of Q , facilitating the forgetting of the unlearned dataset.

Erase: Neighborhood-Aware Parameter Editing

Despite the above analysis theoretically guaranteeing the effectiveness of the masking strategy in achieving unlearning, it has two major limitations. First, the masking strategy overlook the extent to which $\frac{F_{D_f,jj}}{F_{D,jj}}$ exceeds c . In particular, parameters for which $\frac{F_{D_f,jj}}{F_{D,jj}}$ significantly exceeds c are much

more critical for the unlearned dataset compared to those where $\frac{F_{D_f, jj}}{F_{D, jj}}$ only slightly exceeds c . Second, the masking strategy overlooks the impact of unlearned samples on their neighbors through message propagation.

To address the above limitations, we propose the Erase strategy as follows:

$$\widehat{\omega}_{r, j} = \begin{cases} a \frac{F_{D, jj}}{F_{D_f, jj}} \omega_j^*, & F_{D_f, jj} > \gamma F_{D, jj}, \\ b \frac{F_{D, jj}}{F_{D_f, jj} F_{D_k, jj}} \omega_j^*, & F_{D_f, jj} F_{D_k, jj} > \eta F_{D, jj}^2 \\ & \text{and } F_{D_f, jj} \leq \gamma F_{D, jj}, \\ \omega_j^*, & \text{otherwise.} \end{cases} \quad (5)$$

where a , b , γ , and η are hyperparameters.

The advantages of the above design are threefold. First, it considers the impact of unlearned samples on their neighbors. According to the properties of the FIM, a large ratio of $\frac{F_{D_f, jj}}{F_{D, jj}}$ or $\frac{F_{D_k, jj}}{F_{D, jj}}$ indicates that the parameter is crucial for D_f or D_k , but not for D . Drawing inspiration from Theorem 1, if a parameter is crucial for both D_f and D_k , but not for other samples, i.e., satisfying $F_{D_f, jj} F_{D_k, jj} > \eta F_{D, jj}^2$, we consider that the parameter has been influenced by message propagation from D_f . In such cases, we modify these parameters to forget the influence of unlearned samples.

Second, when modifying parameters, we account for the extent to which they are influenced by unlearned samples. Specifically, rather than directly masking the parameters, we use the coefficients $\frac{F_{D, jj}}{F_{D_f, jj}}$ and $\frac{F_{D, jj}}{F_{D_f, jj} F_{D_k, jj}}$ to determine the degree of modification. This implies that a large $\frac{F_{D_f, jj}}{F_{D, jj}}$ or $\frac{F_{D_f, jj} F_{D_k, jj}}{F_{D, jj}^2}$ necessitates substantial modifications to ω_j^* , while a small value requires only minor modifications.

Finally, we balance the two forgetting objectives: forgetting D_f and forgetting the influence of D_f on D_k . One of these objectives may dominate the other due to the potential difference in magnitude between $\frac{F_{D, jj}}{F_{D_f, jj}}$ and $\frac{F_{D, jj}}{F_{D_f, jj} F_{D_k, jj}}$. To mitigate this, we introduce two balancing coefficients a and b to balance these two forgetting objectives.

Note the choice of hyperparameters may vary depending on the dataset. To facilitate hyperparameter selection, we adaptively select them for different datasets. Specifically, γ is set as the top $m\%$ value of $\frac{F_{D_f}}{F_D}$, and η is set as the top $m\%$ value of $\frac{F_{D_f} F_{D_k}}{F_D^2}$. This ensures that $m\%$ of the parameters satisfy $F_{D_f, jj} > \gamma F_{D, jj}$ and $m\%$ satisfy $F_{D_f, jj} F_{D_k, jj} > \eta F_{D, jj}^2$. Furthermore, we set $a = \gamma$ and $b = \eta$ to balance the magnitude between $\frac{F_{D, jj}}{F_{D_f, jj}}$ and $\frac{F_{D, jj}}{F_{D_f, jj} F_{D_k, jj}}$.

Rectify: Model Utility Enhancement

Although the Erase strategy mitigates the impact on the model's predictive performance by considering the extent to which unlearned samples influence parameters, the parameter editing approach may still negatively affect the GNN's performance on D_r to some degree. In this part, we propose

Algorithm 1: ETR: Erase then Rectify

Input: Unlearned dataset D_f ; Dataset D_k ; GNN f_G ; Optimal parameters ω^* ; Gradient $\nabla_{\omega^*} L_D$; Hyperparameters m and λ .

Erase

- 1: Calculate the gradients $\nabla_{\omega^*} L_{D_f}$ and $\nabla_{\omega^*} L_{D_k}$.
- 2: Calculate the FIM F_D, F_{D_f}, F_{D_k} via (2).
- 3: Obtain $\gamma = \text{top-}m\%(\frac{F_{D_f}}{F_D})$ and $\eta = \text{top-}m\%(\frac{F_{D_f} F_{D_k}}{F_D^2})$

4: **for** j in range $|\omega|$ **do**

5: Obtain $\alpha_j = \frac{F_{D_f, jj}}{F_{D_f, jj}}$ and $\beta_j = \frac{F_{D, jj}}{F_{D_f, jj} F_{D_k, jj}}$

6: **if** $F_{D_f, jj} > \gamma F_{D, jj}$ **then**

7: $\widehat{\omega}_{r, j} = \alpha_j \gamma \omega_j^*$

8: **else if** $F_{D_f, jj} F_{D_k, jj} > \eta F_{D, jj}^2$ **then**

9: $\widehat{\omega}_{r, j} = \beta_j \eta \omega_j^*$

10: **else**

11: $\widehat{\omega}_{r, j} = \omega_j^*$

12: **end if**

13: **end for**

Rectify

14: Calculate the gradient $\nabla_{\widehat{\omega}_r} L_{D_k}$.

15: Obtain the gradient $\nabla_{\widehat{\omega}_r} L_{D_r}$ via (9).

16: Obtain the parameters ω' via (10).

Output: ω' .

the Rectify strategy to enhance GNN performance on D_r without requiring access to the entire training dataset, which minimizes computational overhead while ensuring data privacy and security.

Firstly, we estimate the gradients of the edited model on D_r using the induced graph of D_f . Specifically, we assume that we can store the gradients from the model's final iteration of the training phase. After removing D_f , the neighbor structure of $D_r \setminus D_k$ remains unchanged, while only the neighbor structures of D_f and D_k undergo changes. Additionally, during the Erase stage, the modified parameters are crucial only for D_f and D_k , but not for $D_r \setminus D_k$. Therefore, for nodes in $D_r \setminus D_k$, their gradients can be considered nearly unchanged, i.e.,

$$\nabla_{\widehat{\omega}_r} l_j \approx \nabla_{\omega^*} l_j, \forall j \in D_r \setminus D_k \quad (6)$$

where l_j denotes the loss of the GNN on the j -th sample. Through the aforementioned approximation, we can easily calculate the gradient of the edited model on D_r as follows:

$$\nabla_{\widehat{\omega}_r} L_{D_r} = \frac{1}{|D_r|} \sum_{j \in D_r} \nabla_{\widehat{\omega}_r} l_j \quad (7)$$

$$\approx \frac{1}{|D_r|} \left(\sum_{j \in D_r \setminus D_k} \nabla_{\omega^*} l_j + \sum_{j \in D_k} \nabla_{\widehat{\omega}_r} l_j \right) \quad (8)$$

where L_D denotes the loss function of the GNN on dataset D . Further, leveraging the gradient of the GNN on D , we obtain $\sum_{j \in D_r \setminus D_k} \nabla_{\omega^*} l_j = |D| \nabla_{\omega^*} L_D - \sum_{j \in D_f} \nabla_{\omega^*} l_j - \sum_{j \in D_k} \nabla_{\omega^*} l_j$. Finally, we estimate the gradient of the edited model on D_r as follows:

$$\nabla_{\widehat{\omega}_r} L_{D_r} = \frac{1}{|D_r|} (|D| \nabla_{\omega^*} L_D - |D_f| \nabla_{\omega^*} L_{D_f} - |D_k| \nabla_{\omega^*} L_{D_k} + |D_k| \nabla_{\widehat{\omega}_r} L_{D_k}) \quad (9)$$

Backbone	Method	PubMed		CiteSeer		Cora		CS		Physics	
		F1	T								
GCN	Retrain	89.74±0.27	39.1	76.76±0.72	14.1	84.35±1.14	7.5	92.63±0.30	285.8	95.90±0.10	856.7
	BEKM	80.03±0.72	68.2	61.11±2.27	12.7	66.42±3.33	11.0	89.03±0.49	71.7	94.53±0.19	152.7
	BLPA	81.63±0.83	66.1	57.69±2.31	13.0	61.51±3.48	11.5	88.88±0.56	68.2	94.45±0.24	142.8
	GIF	73.66±0.26	0.4	62.88±1.34	<u>0.2</u>	75.87±1.86	<u>0.2</u>	85.19±0.56	1.3	91.37±0.23	3.3
	SR	88.04±0.25	29.0	75.35±0.70	8.6	81.25±0.95	8.6	91.77±0.28	49.0	94.72±0.14	166.4
	Fast	88.11±0.24	29.1	75.83±0.88	8.8	80.70±1.70	8.4	91.64±0.29	47.8	94.74±0.16	138.3
	MEGU	88.26±0.47	0.3	76.04±0.93	<u>0.2</u>	82.62±1.05	<u>0.2</u>	92.39±0.51	0.5	95.40±0.20	0.9
	ETR	89.48±0.34	0.02	77.09±0.60	0.02	83.54±0.92	0.02	92.72±0.37	0.04	95.71±0.15	0.07
GAT	Retrain	88.42±0.36	50.2	76.52±1.00	16.3	82.29±1.00	9.0	92.57±0.43	295.47	96.26±0.18	875.2
	BEKM	70.30±0.77	102.2	49.64±1.36	23.5	56.79±4.83	20.7	81.10±1.39	114.3	92.04±0.43	214.5
	BLPA	71.65±0.78	98.2	49.52±2.44	20.1	49.70±3.17	18.7	81.35±0.58	94.2	91.82±0.43	194.5
	GIF	88.07±0.22	1.1	75.80±1.06	0.7	81.70±1.38	0.6	92.79±0.36	2.1	<u>95.84±0.16</u>	5.1
	SR	86.67±0.41	33.6	75.92±0.88	12.0	76.05±1.78	12.3	89.49±0.64	54.8	94.76±0.41	149.3
	Fast	86.60±0.33	35.4	75.89±0.93	12.4	75.46±0.93	12.3	89.70±0.95	55.3	94.86±0.45	145.5
	MEGU	85.23±0.47	0.3	76.07±0.79	<u>0.2</u>	82.84±0.72	<u>0.2</u>	91.74±0.32	0.6	95.14±0.22	<u>1.2</u>
	ETR	88.32±0.22	0.03	76.31±1.59	0.03	79.70±0.85	0.03	92.45±0.13	0.05	96.19±0.18	0.09

Table 1: Performance comparison in terms of F1 score and running time, where F1 indicates the F1 score, T indicates the running time (in seconds). The best experimental results are highlighted in bold, while the second-best results are underscored.

Notably, $\nabla_{\omega^*} L_D$ can be stored during GNN training, while the sizes of D_f and D_k are typically small. Therefore, we can efficiently approximate $\nabla_{\hat{\omega}_r} L_{D_r}$ through (9). After obtaining the gradient $\nabla_{\hat{\omega}_r} L_{D_r}$, we rectify the parameters through one-step gradient descent, defined as follows:

$$\omega' = \hat{\omega}_r - \lambda \nabla_{\hat{\omega}_r} L_{D_r} \quad (10)$$

where λ is the hyperparameter. The pseudo-code for the ETR approach is presented in Algorithm 1.

For edge and feature unlearning, we can forget the impact of the unlearned edges or features and enhance model performance in a similar manner. The pseudo-code for edge and feature unlearning is provided in the Appendix.

Complexity Analysis

In this section, we analyze the complexity of ETR. Calculating $\nabla_{\omega^*} L_{D_f}$ with a time complexity of $\mathcal{O}(|D_f|)$. Similarly, calculating $\nabla_{\omega^*} L_{D_k}$ and $\nabla_{\hat{\omega}_r} L_{D_k}$ with a time complexity of $\mathcal{O}(|D_k|)$. Computing the FIM has a time complexity of $\mathcal{O}(|\omega|)$. The Erase strategy can be executed in parallel, with a time complexity of $\mathcal{O}(|\omega|)$. Thus, the overall time complexity of ETR is $\mathcal{O}(|D_f| + |D_k| + |\omega|)$. Regarding space complexity, the GNN parameters have a space complexity of $\mathcal{O}(|\omega|)$. The node features have a space complexity of $\mathcal{O}(|D_f|d + |D_k|d)$. The edges have a space complexity of $\mathcal{O}(|\mathcal{E}_f| + |\mathcal{E}_k|)$, where $|\mathcal{E}_f|$ and $|\mathcal{E}_k|$ denote the number of edges in D_f and D_k , respectively. Computing the FIM has a space complexity of $\mathcal{O}(|\omega|)$. Therefore, the overall space complexity of ETR is $\mathcal{O}(|D_f|d + |D_k|d + |\omega| + |\mathcal{E}_f| + |\mathcal{E}_k|)$. Notably, D_f and D_k are much smaller than D , resulting in low computational overhead for large-scale graphs.

Experiments

In this section, we conduct extensive experiments to evaluate the effectiveness of ETR. The experiments aim to answer the following research questions: **RQ1**: How does ETR perform

in terms of model utility, unlearning efficiency, and unlearning efficacy? **RQ2**: How does ETR perform on large-scale graphs? **RQ3**: How do hyperparameters influence ETR’s performance? **RQ4**: How do different strategies in ETR contribute to its effectiveness?

Experimental Setup

Datasets We conduct experiments on PubMed, CiteSeer, Cora (Yang, Cohen, and Salakhutdinov 2016), CS, Physics (Shchur et al. 2018), ogbn-arxiv, and ogbn-products (Hu et al. 2020). The statistics and detailed descriptions of these datasets are provided in the Appendix.

Baselines We compare ETR with various baselines, including Retrain, GraphEraser-BEKM, GraphEraser-BLPA (Chen et al. 2022), GIF (Wu et al. 2023a), GUIDE-SR, GUIDE-Fast (Wang, Huai, and Wang 2023), and MEGU (Li et al. 2024). Detailed descriptions of these baselines are provided in the Appendix.

Settings Following GIF, we partition each graph into a training subgraph comprising training nodes and a test subgraph containing the remaining nodes. For PubMed, CiteSeer, Cora, CS, and Physics, we randomly allocate 90% of the nodes to the training set. For ogbn-arxiv and ogbn-products, we use the splits provided in (Hu et al. 2020). The unlearning ratio is set to 5% for all tasks. We use two-layer GCN and GAT models with a hidden state dimension of 256, training for 100 epochs. All experiments are conducted on a single Nvidia A40 GPU. Each experiment is run ten times, and we report the average value and standard deviation.

Evaluation of Model Utility (RQ1)

We evaluate the F1 score for node classification on the remaining dataset. The results for node unlearning are shown in Table 1, while the results for edge and feature unlearning are provided in the Appendix. It can be observed that ETR

Backbone	Method	PubMed	CiteSeer	Cora	CS	Physics
GCN	Retrain	1.57	1.52	1.3	6.13	14.62
	BEKM	0.8	0.6	0.45	5.87	14.87
	BLPA	0.45	0.48	0.38	1.44	2.89
	GIF	1.7	1	0.61	11.18	37.63
	SR	1.48	1.23	1.2	2.09	4.97
	Fast	1.44	1.23	1.2	2.36	5.1
	MEGU	0.68	0.52	0.41	2.07	4.52
	ETR	1.18	1.21	1.17	1.61	2.43
GAT	Retrain	1.77	1.52	1.3	6.17	15.28
	BEKM	0.78	0.6	0.45	5.87	14.86
	BLPA	0.48	0.48	0.4	1.6	3.53
	GIF	2.88	0.8	0.72	5.89	14.3
	SR	1.52	1.23	1.2	2.2	5.21
	Fast	1.52	1.23	1.2	2.41	5.32
	MEGU	0.94	0.57	0.45	3.62	7.64
	ETR	1.2	1.21	1.17	1.54	2.3

Table 2: The memory overhead (GB) of different methods.

Backbone	Method	PubMed	CiteSeer	Cora	CS	Physics
GCN	BEKM	5e-2	2e-3	8e-3	2e-2	2e-2
	BLPA	5e-2	2e-3	8e-3	2e-2	1e-2
	GIF	7e-2	4e-3	2e-2	3e-2	1e-2
	SR	9e-2	8e-3	2e-2	8e-3	2e-3
	Fast	8e-2	9e-3	2e-2	8e-3	2e-3
	MEGU	1e-2	3e-3	3e-2	1e-3	7e-4
	ETR	3e-2	5e-4	9e-4	4e-4	2e-4
	GAT	BEKM	9e-3	1e-2	2e-2	9e-3
BLPA		9e-3	1e-2	2e-2	8e-3	5e-4
GIF		6e-2	7e-3	2e-2	2e-3	3e-2
SR		7e-2	1e-2	1e-2	4e-3	7e-2
Fast		7e-2	1e-2	1e-2	4e-3	7e-2
MEGU		9e-2	4e-2	3e-3	2e-2	1e-2
ETR		3e-2	1e-3	2e-3	4e-4	2e-4

Table 3: The root mean square distance between the parameters and those of Retrain.

consistently performs best in most cases, which can be attributed to the Rectify strategy that enhances model performance on the remaining dataset. Additionally, BEKM and BLPA exhibit suboptimal performance, consistent with the results reported in their original papers, likely due to disruptions in graph structure resulting from graph partitioning. GUIDE mitigates this problem, leading to improved performance. Among the baselines, MEGU achieves the best performance, which can be attributed to its training of the model’s predictive objective during unlearning.

Evaluation of Unlearning Efficiency (RQ1)

The runtime results are presented in Table 1. ETR consistently outperforms all baselines, which can be attributed to its training-free nature. ETR reduces runtime by thousands of times compared to Retrain, demonstrating its superior efficiency. While GraphEraser and GUIDE are also faster than Retrain in most cases, they still require considerable time for unlearning due to the need for retraining multiple models. Although GIF and MEGU improve runtime efficiency compared to other baselines, they still fall short of ETR. Specifically, ETR reduces runtime by 38 times compared to GIF

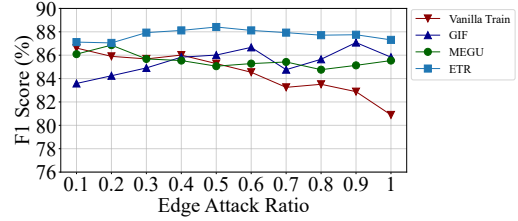


Figure 2: Adversarial edge unlearning on the Cora dataset.

Bone	Method	ogbn-arxiv				ogbn-products			
		F1	T	S	D	F1	T	S	D
GCN	Retrain	67.5	152	3.7	-	73.6	519	11.2	-
	BEKM	64.8	1290	2.9	8e-1	OM	OM	OM	OM
	BLPA	63.9	1323	0.9	8e-1	OM	OM	OM	OM
	GIF	62.1	7	19.7	1	OM	OM	OM	OM
	MEGU	65.6	2	5.9	4e-2	71.3	7	26.8	6e-2
	ETR	66.4	0.08	1.2	2e-2	73.8	0.5	1.2	9e-3
GAT	Retrain	67.3	217.9	6	-	73.9	709	11.2	-
	BEKM	65.3	1804	3.0	6e-1	OM	OM	OM	OM
	BLPA	64.7	1658	2.5	6e-1	OM	OM	OM	OM
	GIF	66.1	12	34.5	5e-1	OM	OM	OM	OM
	MEGU	58.5	3	11.2	4e-3	63.7	8	26.9	5e-2
	ETR	67.8	0.1	1	2e-2	73.9	0.7	1.3	2e-2

Table 4: Performance comparison on large-scale graphs, where S denotes memory overhead, D indicates parameter distance, and “OM” represents “out of memory”.

and 12 times compared to MEGU.

The memory overhead results are shown in Table 2. ETR performs comparably to the baselines on small datasets and outperforms them on larger datasets (Photo and Computer). This is because memory overhead on small datasets is primarily driven by model parameters, limiting the advantages of ETR. However, ETR reduces memory overhead on large datasets by not requiring the entire training dataset, decreasing it by 3.4 times compared to Retrain. Among the baselines, BLPA performs best due to its use of graph partitioning, which reduces memory overhead but significantly degrades model utility. Overall, ETR achieves an excellent trade-off between unlearning efficiency and model utility.

Evaluation of Unlearning Efficacy (RQ1)

We assess unlearning efficacy using both direct and indirect evaluation methods. For direct evaluation, we measure the root mean square distance between the parameters of the unlearned model and those of the retrained model. As shown in Table 3, ETR consistently performs best in most cases, indicating that its parameters are closest to those obtained by retraining from scratch, thereby demonstrating ETR’s effectiveness in achieving graph unlearning.

For indirect evaluation, we follow the approach used by GIF and MEGU, adding adversarial edges between nodes of different categories in the training graph. These edges serve as unlearning targets, and we then assess the utility of the unlearned model. As shown in Figure 2, the performance of the vanilla trained model declines with increasing attack ra-

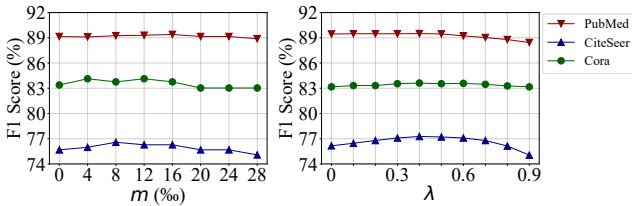


Figure 3: Performance with varying hyperparameters.

tios, while GIF, MEGU, and ETR maintain or even improve performance. This demonstrates the effectiveness of these methods. Notably, ETR consistently outperforms the other baselines, highlighting its strong unlearning efficacy.

Evaluation on Large Scale Graphs (RQ2)

We conduct experiments on the ogbn-arxiv and ogbn-products datasets to assess ETR’s effectiveness and efficiency on large-scale graphs, with the results shown in Table 4. GUIDE encounters out-of-memory issues on both datasets, while GraphEraser and GIF also experience out-of-memory issues on the ogbn-products dataset. ETR demonstrates superior performance in terms of model utility, unlearning efficiency, and unlearning efficacy on large-scale graphs. Specifically, ETR shows an average utility improvement of 9.13% over MEGU, reduces runtime by thousands of times compared to Retrain, and decreases memory overhead by 7 times compared to Retrain and 15 times compared to MEGU. In terms of unlearning efficacy, ETR performs best in most cases. Overall, ETR achieves better performance and efficiency compared to other methods.

Hyperparameter Analysis (RQ3)

The hyperparameters m and λ are crucial for ETR’s performance. The value of m determines how much the parameters are modified, thereby influencing the extent of model forgetting. The value of λ controls the extent of model rectification. In this section, we investigate their impact on ETR’s performance using the PubMed, CiteSeer, and Cora datasets.

We investigate how different values of m affect the performance of the Erase strategy, with results shown in Figure 3. It can be observed that increasing m generally improves model performance, but performance declines if m becomes too large. This is because larger m values help the model forget unlearned samples effectively, while excessively large values can also lead to the loss of essential knowledge. Typically, m values between 8% and 16% provide the best results for the Erase strategy. Notably, the model performs better compared to $m = 0$, confirming that the Erase strategy effectively forgets unlearned samples and supports Theorem 1.

We tune λ within the range of $[0, 0.9]$ to investigate how it affects ETR’s performance, with results shown in Figure 3. It can be observed that ETR’s performance generally improves as λ increases. However, performance declines if λ becomes too large. This is because larger λ values aid in model rectification, while excessively large values can also lead to exces-

Method	PubMed	CiteSeer	Cora	CS	Physics
w/ mask	88.91	77.00	82.51	92.44	95.80
w/o mes	89.30	76.91	82.44	92.53	95.70
ETR	89.48	77.09	83.54	92.72	95.71

Table 5: Performance comparison between model variants.

Metric	PubMed	CiteSeer	Cora	CS	Physics
AD	5.7E-06	8.1E-07	1.7E-06	5.3E-06	1.6E-04
RD	0.23	0.09	0.07	0.36	0.22

Table 6: The difference between the approximate gradient and the true gradient.

sive rectification. Optimal performance for ETR is typically achieved with λ values between 0.3 and 0.5.

Ablation Studies (RQ4)

In this section, we investigate the effectiveness of different strategies in ETR. The Erase is crucial for model forgetting, while the Rectify is critical for maintaining model utility. The results in Figure 3 indicate that increasing m improves performance compared to $m = 0$, demonstrating the effectiveness of the Erase strategy in forgetting the unlearned samples. The results in Figure 3 show that increasing λ also improves performance compared to $\lambda = 0$, indicating that the Rectify strategy effectively enhances the model performance on the remaining dataset.

To further investigate the effectiveness of the Erase strategy, we compare ETR with two model variants, as shown in Table 5. Specifically, “w/ mask” refers to using the masking strategy, while “w/o mes” indicates not considering the impact of message propagation. The results show that ETR outperforms both variants in most cases, except for a slight decrease on the Physics dataset compared to “w/ mask”. This demonstrates that parameter editing is more effective than just applying a mask and emphasizes the importance of considering message propagation in graph unlearning.

In the Rectify stage, we use the induced graph of unlearned samples to approximate the gradient of the model on the remaining dataset. We measure the difference of this approximation using Absolute Difference (AD) and Relative Difference (RD), as shown in Table 6. The results show that both differences are minimal, indicating that the gradient approximation ensures both efficiency and accuracy.

Conclusion

In this paper, we investigate cost-effective graph unlearning and propose a training-free approach ETR to remove the influence of unlearned samples while maintaining the model performance on the remaining dataset. Specifically, in the Erase stage, we utilize the Fisher Information Matrix to identify parameters crucial for unlearned samples and their influence on other inter-connected samples. These parameters are then modified to forget the unlearned samples and their effects on other samples through message propagation. In the Rectify stage, we use the induced graph of the unlearned samples to efficiently approximate the model’s gra-

dient on the remaining dataset. This gradient is then used to enhance the model performance on the remaining data. Extensive experiments on seven public datasets demonstrate that the proposed ETR method achieves an excellent trade-off between efficiency and effectiveness.

References

- Bourtole, L.; Chandrasekaran, V.; Choquette-Choo, C. A.; Jia, H.; Travers, A.; Zhang, B.; Lie, D.; and Papernot, N. 2021. Machine Unlearning. In *SP*, 141–159.
- Chen, C.; Zheng, S.; Chen, X.; Dong, E.; Liu, X. S.; Liu, H.; and Dou, D. 2021. Generalized Data Weighting via Class-Level Gradient Manipulation. In *NeurIPS*, 14097–14109.
- Chen, M.; Zhang, Z.; Wang, T.; Backes, M.; Humbert, M.; and Zhang, Y. 2022. Graph Unlearning. In *CCS*, 499–513.
- Chen, Z.; Li, P.; Liu, H.; and Hong, P. 2023. Characterizing the Influence of Graph Elements. In *ICLR*.
- Cheng, J.; Dasoulas, G.; He, H.; Agarwal, C.; and Zitnik, M. 2023. GNNDelete: A General Strategy for Unlearning in Graph Neural Networks. In *ICLR*.
- Chien, E.; Pan, C.; and Milenkovic, O. 2023. Efficient Model Updates for Approximate Unlearning of Graph-Structured Data. In *ICLR*.
- Foster, J.; Schoepf, S.; and Brintrup, A. 2024. Fast Machine Unlearning without Retraining through Selective Synaptic Dampening. In *AAAI*, 12043–12051.
- Gilmer, J.; Schoenholz, S. S.; Riley, P. F.; Vinyals, O.; and Dahl, G. E. 2017. Neural Message Passing for Quantum Chemistry. In *ICML*, 1263–1272.
- Golatkar, A.; Achille, A.; and Soatto, S. 2020a. Eternal Sunshine of the Spotless Net: Selective Forgetting in Deep Networks. In *CVPR*, 9301–9309.
- Golatkar, A.; Achille, A.; and Soatto, S. 2020b. Forgetting Outside the Box: Scrubbing Deep Networks of Information Accessible from Input-Output Observations. In *ECCV (29)*, 383–398.
- Guo, C.; Goldstein, T.; Hannun, A. Y.; and van der Maaten, L. 2020. Certified Data Removal from Machine Learning Models. In *ICML*, 3832–3842.
- Hu, W.; Fey, M.; Zitnik, M.; Dong, Y.; Ren, H.; Liu, B.; Catasta, M.; and Leskovec, J. 2020. Open Graph Benchmark: Datasets for Machine Learning on Graphs. In *NeurIPS*.
- Kay, S. M. 1993. *Fundamentals of statistical signal processing: estimation theory*. Prentice-Hall, Inc.
- Kipf, T. N.; and Welling, M. 2017. Semi-Supervised Classification with Graph Convolutional Networks. In *ICLR (Poster)*.
- Kirkpatrick, J.; Pascanu, R.; Rabinowitz, N.; Veness, J.; Desjardins, G.; Rusu, A. A.; Milan, K.; Quan, J.; Ramalho, T.; Grabska-Barwinska, A.; Hassabis, D.; Clopath, C.; Kumaran, D.; and Hadsell, R. 2017. Overcoming catastrophic forgetting in neural networks. *Proceedings of the National Academy of Sciences*, 114(13): 3521–3526.
- Li, X.; Zhao, Y.; Wu, Z.; Zhang, W.; Li, R.; and Wang, G. 2024. Towards Effective and General Graph Unlearning via Mutual Evolution. In *AAAI*, 13682–13690.
- Maini, P.; Mozer, M. C.; Sedghi, H.; Lipton, Z. C.; Kolter, J. Z.; and Zhang, C. 2023. Can Neural Network Memorization Be Localized? In *ICML*, 23536–23557.
- Nguyen, T. T.; Huynh, T. T.; Nguyen, P. L.; Liew, A. W.; Yin, H.; and Nguyen, Q. V. H. 2022. A Survey of Machine Unlearning. *CoRR*, abs/2209.02299.
- Said, A.; Derr, T.; Shabbir, M.; Abbas, W.; and Koutsoukos, X. D. 2023. A Survey of Graph Unlearning. *CoRR*, abs/2310.02164.
- Shchur, O.; Mumme, M.; Bojchevski, A.; and Günnemann, S. 2018. Pitfalls of Graph Neural Network Evaluation. *CoRR*, abs/1811.05868.
- Tarun, A. K.; Chundawat, V. S.; Mandal, M.; and Kankanhalli, M. 2023. Fast Yet Effective Machine Unlearning. *IEEE Transactions on Neural Networks and Learning Systems*, 1–10.
- Velickovic, P.; Cucurull, G.; Casanova, A.; Romero, A.; Liò, P.; and Bengio, Y. 2018. Graph Attention Networks. In *ICLR (Poster)*.
- Wang, C.; Huai, M.; and Wang, D. 2023. Inductive Graph Unlearning. In *USENIX Security Symposium*, 3205–3222.
- Wu, J.; Yang, Y.; Qian, Y.; Sui, Y.; Wang, X.; and He, X. 2023a. GIF: A General Graph Unlearning Strategy via Influence Function. In *WWW*, 651–661.
- Wu, K.; Shen, J.; Ning, Y.; Wang, T.; and Wang, W. H. 2023b. Certified Edge Unlearning for Graph Neural Networks. In *KDD*, 2606–2617.
- Xu, H.; Zhu, T.; Zhang, L.; Zhou, W.; and Yu, P. S. 2024. Machine Unlearning: A Survey. *ACM Comput. Surv.*, 56(1): 9:1–9:36.
- Yang, Z.; Cohen, W. W.; and Salakhutdinov, R. 2016. Revisiting Semi-Supervised Learning with Graph Embeddings. In *ICML*, 40–48.
- Zhou, J.; Cui, G.; Hu, S.; Zhang, Z.; Yang, C.; Liu, Z.; Wang, L.; Li, C.; and Sun, M. 2020. Graph neural networks: A review of methods and applications. *AI Open*, 1: 57–81.

Theoretical Analysis

Prior to proving Theorem 1, we first introduce some notation that will be used in the proof. Considering the architectural differences among various GNNs, for the sake of simplicity in our analysis, we consider the following general two-layer GNN architecture:

$$H_1 = \sigma(PXW_0) \quad (11)$$

$$H_2 = PH_1W_1 \quad (12)$$

$$Z = \text{softmax}(H_2) \quad (13)$$

where P represents the message transformation matrix associated with the adjacency matrix, $\sigma(\cdot)$ denotes the activation function, W_0 and W_1 represent parameter matrices. In the node classification task, the loss function is given by:

$$L = -\frac{1}{|D|} \sum_{i \in D} \sum_{j=1}^C Y_{i,j} \log(Z_{i,j}). \quad (14)$$

Based on the definition of the Fisher Information Matrix, the following properties are established:

$$F_D = \frac{1}{|D|} \sum_{i=1}^{|D|} \nabla_w \log p(y_i|x_i, w) \nabla_w \log p(y_i|x_i, w)^T \quad (15)$$

$$= \frac{1}{|D|} \sum_{i \in D_f} \nabla_w \log p(y_i|x_i, w) \nabla_w \log p(y_i|x_i, w)^T \quad (16)$$

$$+ \frac{1}{|D|} \sum_{i \in D_r} \nabla_w \log p(y_j|x_j, w) \nabla_w \log p(y_j|x_j, w)^T \quad (17)$$

$$= \frac{|D_f|}{|D|} F_{D_f} + \frac{|D_r|}{|D|} F_{D_r}. \quad (18)$$

We denote the vectorization of the matrix W as $\text{vec}(W)$ and define $\omega = \text{vec}(W_0, W_1) = \text{concat}(\text{vec}(W_0), \text{vec}(W_1))$, where $\text{concat}(\cdot, \cdot)$ denotes the concatenation of two vectors. We now present the proof of Theorem 1.

Proof of Theorem 1. First, we compute the gradients of the backpropagation using the node classification loss function as follows:

$$\frac{\partial L}{\partial W_1} = H_1^T P^T (Z - Y) \quad (19)$$

$$\frac{\partial L}{\partial W_0} = X^T P^T \left\{ [(Z - Y) W_1^T P^T] \odot \sigma'(PXW_0) \right\} \quad (20)$$

According to the definition of the Fisher Information Matrix, we have: $F = \text{vec} \left(\frac{\partial L}{\partial W_1}, \frac{\partial L}{\partial W_0} \right) \text{vec} \left(\frac{\partial L}{\partial W_1}, \frac{\partial L}{\partial W_0} \right)^T$. For the sake of simplicity, we decompose F by analyzing W_0 and W_1 separately. Define $F_0 = \text{vec} \left(\frac{\partial L}{\partial W_0} \right) \text{vec} \left(\frac{\partial L}{\partial W_0} \right)^T$ and $F_1 = \text{vec} \left(\frac{\partial L}{\partial W_1} \right) \text{vec} \left(\frac{\partial L}{\partial W_1} \right)^T$. Accordingly, we have: $F_1 \text{vec}(W_1) = \text{tr}(H_2(Z - Y)) \text{vec} \left(\frac{\partial L}{\partial W_1} \right)$, and $F_0 \text{vec}(W_0) = \text{tr} \left(W_0 \frac{\partial L}{\partial W_0} \right) \text{vec} \left(\frac{\partial L}{\partial W_0} \right)$. We denote $b := F\omega \approx [F_0W_0; F_1W_1]$

According to Formulation (3), we have:

$$\frac{1}{|\omega|} \sum_j (\omega_{r,j}^* - \hat{\omega}_{r,j})^2 \quad (21)$$

$$= \frac{1}{|\omega|} \left(\sum_{j \in M} \omega_{r,j}^{*2} + \sum_{j \notin M} (\omega_{r,j}^* - \omega_j^*)^2 \right) \quad (22)$$

Using $\text{diag}(F)$ to approximate the Fisher information matrix F , the first term of Formulation (22) is given by:

$$\sum_{j \in M} \omega_{r,j}^{*2} = \sum_{j \in M} \frac{b_{r,j}^2}{F_{D_r,jj}^2} \leq c_1 \sum_{j \in M} \frac{1}{F_{D_r,jj}^2} \quad (23)$$

where $c_1 = \max_j b_{r,j}^2$. And the second term of Formulation (24) is given by:

$$\sum_{j \notin M} (\omega_{r,j}^* - \omega_j^*)^2 \quad (24)$$

$$= \sum_{j \notin M} \left(\frac{b_j}{F_{D,jj}} - \frac{b_{r,j}}{F_{D_r,jj}} \right)^2 \quad (25)$$

$$= \sum_{j \notin M} \left(\frac{b_j F_{D_r,jj} - b_{r,j} F_{D,jj}}{F_{D,jj} F_{D_r,jj}} \right)^2 \quad (26)$$

$$= \sum_{j \notin M} \left(\frac{b_j F_{D_r,jj} - b_{r,j} \frac{|D_f|}{|D|} F_{D_f,jj} - b_{r,j} \frac{|D_r|}{|D|} F_{D_r,jj}}{F_{D,jj} F_{D_r,jj}} \right)^2 \quad (27)$$

$$= \sum_{j \notin M} \left(\left(b_j - b_{r,j} \frac{|D_r|}{|D|} \right) \frac{1}{F_{D,jj}} - b_{r,j} \frac{|D_f|}{|D|} \frac{F_{D_f,jj}}{F_{D_r,jj}} \right)^2 \quad (28)$$

$$\leq \sum_{j \notin M} \left(b_j - b_{r,j} \frac{|D_r|}{|D|} \right)^2 \frac{2}{F_{D,jj}^2} \quad (29)$$

$$+ \sum_{j \notin M} \left(b_{r,j} \frac{|D_f|}{|D|} \right)^2 \frac{F_{D_f,jj}^2}{F_{D,jj}^2 F_{D_r,jj}^2} \quad (30)$$

$$\leq c_2 \sum_{j \notin M} \frac{F_{D_f,jj}^2}{F_{j,j}^2 F_{r,jj}^2} + c_3 \quad (31)$$

where $c_2 = \max_j \left(b_{r,j} \frac{|D_f|}{|D|} \right)^2$, and $c_3 = \sum_j \left(b_j - b_{r,j} \frac{|D_r|}{|D|} \right)^2 \frac{2}{F_{D,jj}^2}$.

Therefore, we can obtain:

$$\frac{1}{|\omega|} \sum_j (\omega_{r,j}^* - \hat{\omega}_{r,j})^2 \quad (32)$$

$$= \frac{1}{|\omega|} \left(\sum_{j \in M} \omega_{r,j}^{*2} + \sum_{j \notin M} (\omega_{r,j}^* - \omega_j^*)^2 \right) \quad (33)$$

$$\leq \frac{1}{|\omega|} \left(c_1 \sum_{j \in M} \frac{1}{F_{D_r,jj}^2} + c_2 \sum_{j \notin M} \frac{F_{D_f,jj}^2}{F_{D,jj}^2 F_{D_r,jj}^2} + c_3 \right) \quad (34)$$

□

Datasets

Dataset Statistics

Dataset	#Nodes	#Edges	#Features	#Classes
PubMed	19,717	88,651	500	3
CiteSeer	3,327	9,228	3,703	6
Cora	2,708	10,556	1,433	7
CS	18,333	163,788	6,805	15
Physics	34,493	495,924	8,415	5
ogbn-arxiv	169,343	1,166,243	128	40
ogbn-products	2,449,029	61,859,140	100	47

Table 7: Statistics of datasets.

Dataset Descriptions

- **PubMed, CiteSeer, and Cora.** PubMed, CiteSeer, and Cora are three standard citation network benchmark datasets. In these datasets, the nodes correspond to research papers, and the edges represent the citations between papers. The node features are derived from the bag-of-words representation of the papers, while the node labels indicate the academic topics of the papers.
- **CS and Physics.** CS and Physics are two co-authorship networks focused on research papers. In these datasets, nodes represent authors of research papers, while edges denote the co-authorship relationships among them. Node features derive from the keywords associated with each author’s publications, and node labels indicate the most active fields of study for each author.
- **ogbn-arxiv.** ogbn-arxiv is a large-scale citation network comprising Computer Science papers from arXiv. In this dataset, nodes represent individual arXiv papers, while edges signify the citation relationships between them. Node features are generated by averaging the embeddings of the words found in the title and abstract of each paper. Node labels denote the subject areas of the papers.
- **ogbn-products.** ogbn-products is a large-scale co-purchasing network of Amazon products. In this dataset, nodes represent individual products sold on Amazon, while edges indicate pairs of products that were purchased together. Node features are derived by extracting bag-of-words features from product descriptions. Node labels denote the product categories.

Baselines

- **Retrain:** Retrain is an exact graph unlearning method that entails retraining the model from scratch on the remaining dataset upon receiving an unlearning request.
- **GraphEraser:** GraphEraser is the first approximate graph unlearning method, adhering to the SISA paradigm. It partitions the training graph into multiple shards, trains a model on each shard, and subsequently aggregates the various submodels. Upon receiving an unlearning request, only the affected submodels need to be retrained. GraphEraser-BEKM and GraphEraser-BLPA denote the application of different graph partitioning methods.

Algorithm 2: ETR for Edge and Feature Unlearning

Input: Influenced dataset D_i ; GNN f_G ; Optimal parameters ω^* ; Gradient $\nabla_{\omega^*} L_D$; Hyperparameters m and λ .

Erase

- 1: Calculate the gradients $\nabla_{\omega^*} L_{D_i}$.
- 2: Calculate the FIM F_D, F_{D_i} via (2).
- 3: Obtain $\gamma = \text{top-}k\%(\frac{F_{D_i}}{F_D})$.
- 4: **for** j in range $|\omega|$ **do**
- 5: Obtain $\alpha_j = \frac{F_{D_i,jj}}{F_{D_i,jj}}$
- 6: **if** $F_{D_i,jj} > \gamma F_{D_i,jj}$ **then**
- 7: $\hat{\omega}_{r,j} = \alpha_j \gamma \omega_j^*$
- 8: **else**
- 9: $\hat{\omega}_{r,j} = \omega_j^*$
- 10: **end if**
- 11: **end for**

Rectify

- 12: Calculate the gradient $\nabla_{\hat{\omega}_r} L_{D_k}$.
- 13: Obtain the gradient $\nabla_{\hat{\omega}_r} L_{D_r}$ via (36).
- 14: Obtain the parameters ω' via (10).

Output: ω' .

- **GIF:** GIF utilizes influence functions to approximate the parameter changes resulting from an unlearning request. It subsequently updates the model parameters based on these estimated changes to facilitate graph unlearning.
- **GUIDE:** GUIDE is specifically designed for inductive graph unlearning and follows the SISA paradigm. GUIDE takes into account fairness and balance in graph partitioning and addresses the disruptions caused to the graph structure. GUIDE-Fast and GUIDE-SR represent the application of different graph partitioning methods.
- **MEGU:** MEGU integrates the model’s predictive capability and forgetting ability within a unified optimization framework, thereby facilitating mutual benefits between these two objectives.

ETR for Edge Unlearning and Feature Unlearning

For edge and feature unlearning, it is necessary to forget the impact of the unlearned edges or features on other nodes. We denote the subgraph affected by the unlearned edges or features as D_i . Consequently, we modify the parameters that are crucial for D_i but not for the remaining dataset, as detailed in Algorithm 2. Additionally, we approximate the gradient of the model on the remaining dataset as follows:

$$\nabla_{\hat{\omega}_r} L_{D_r} = \frac{1}{|D_r|} (|D| \nabla_{\omega^*} L_D - |D_i| \nabla_{\omega^*} L_{D_i} + \quad (35)$$

$$|D_i| \nabla_{\hat{\omega}_r} L_{D_i}) \quad (36)$$

Furthermore, we utilize this gradient to enhance the model performance on the remaining dataset, as demonstrated in Algorithm 2.

Additional Experimental Results

Backbone	Method	PubMed	CiteSeer	Cora	CS	Physics	ogbn-arxiv
GCN	Retrain	89.95±0.18	78.17±0.84	86.64±0.54	93.48±0.23	96.45±0.18	68.07±1.38
	BEKM	78.90±0.48	59.85±1.70	65.68±3.01	87.62±0.64	94.66±0.37	64.90±0.25
	BLPA	80.52±0.44	56.52±2.86	60.66±2.90	87.48±0.74	94.46±0.34	63.60±0.56
	GIF	83.20±0.22	72.55±1.06	82.62±1.38	92.62±0.36	95.61±0.16	65.76±1.06
	SR	87.36±0.28	78.26±0.79	84.46±0.93	92.14±0.14	94.91±0.12	OOM
	Fast	87.36±0.24	<u>78.44±0.87</u>	84.65±0.89	92.14±0.17	94.95±0.12	OOM
	MEGU	<u>87.81±0.23</u>	77.27±0.81	<u>86.53±0.80</u>	<u>93.23±0.40</u>	96.01±0.11	66.97±1.67
	ETR	89.88±0.21	79.28±0.76	87.23±0.76	93.48±0.26	96.43±0.16	68.10±0.63
GAT	Retrain	88.60±0.26	77.66±0.91	84.13±1.44	93.08±0.17	96.65±0.11	69.03±0.60
	BEKM	70.01±0.91	53.48±2.34	48.93±2.70	82.19±0.47	91.09±0.44	64.79±0.22
	BLPA	71.26±1.17	51.59±2.86	49.89±6.71	81.80±0.62	90.83±0.27	64.37±0.26
	GIF	<u>88.04±0.33</u>	<u>76.91±1.35</u>	<u>85.06±1.18</u>	93.59±0.22	<u>96.26±0.19</u>	<u>67.49±1.46</u>
	SR	85.74±0.49	76.25±0.85	79.82±1.54	90.51±0.68	94.46±0.98	OOM
	Fast	85.81±0.64	75.65±0.86	79.45±2.01	90.60±0.76	93.81±1.31	OOM
	MEGU	84.24±0.40	75.44±0.88	86.61±1.11	92.32±0.31	95.09±0.19	59.69±1.69
	ETR	88.21±0.48	77.87±0.93	84.32±0.91	<u>93.40±0.27</u>	96.61±0.17	69.40±0.46

Table 8: Performance comparison in terms of model utility in the edge unlearning task.

Backbone	Method	PubMed	CiteSeer	Cora	CS	Physics	ogbn-arxiv
GCN	Retrain	89.96±0.26	78.35±0.62	87.16±0.42	93.59±0.13	96.55±0.11	68.59±1.27
	BEKM	79.94±0.50	58.26±3.50	60.89±6.51	89.22±0.52	94.67±0.17	65.01±0.24
	BLPA	81.60±0.59	54.17±3.23	61.33±2.85	88.79±0.33	94.58±0.24	63.87±0.33
	GIF	84.60±0.26	73.54±0.48	84.24±1.00	93.06±0.27	95.63±0.13	65.52±1.30
	SR	87.44±0.24	77.03±0.50	78.19±4.21	91.19±0.36	95.00±0.09	OOM
	Fast	87.44±0.35	76.97±0.76	78.23±3.76	91.32±0.21	95.00±0.10	OOM
	MEGU	<u>87.87±0.17</u>	<u>77.60±0.51</u>	<u>85.65±0.71</u>	<u>93.50±0.17</u>	96.01±0.14	66.70±1.95
	EAR	90.17±0.24	78.98±0.71	87.08±0.43	93.63±0.22	96.54±0.11	68.27±0.92
GAT	Retrain	88.52±0.26	77.66±0.79	85.20±0.81	93.25±0.46	96.57±0.20	68.76±0.77
	BEKM	69.31±1.15	52.76±2.92	59.45±3.08	82.52±0.70	91.15±0.41	<u>65.38±0.23</u>
	BLPA	70.84±0.95	48.32±1.71	55.17±3.94	82.72±0.38	91.17±0.36	64.82±0.25
	GIF	<u>88.11±0.37</u>	<u>77.33±1.30</u>	<u>85.35±1.43</u>	<u>93.04±0.22</u>	96.58±0.18	64.38±11.07
	SR	85.65±0.30	75.35±0.87	73.91±3.47	82.55±3.33	91.73±1.89	OOM
	Fast	85.34±0.28	75.83±0.73	73.25±4.07	82.57±4.09	90.36±2.70	OOM
	MEGU	84.20±0.48	75.59±0.91	87.31±1.06	92.24±0.24	95.50±0.14	59.40±1.75
	EAR	88.45±0.41	77.84±0.96	84.58±0.93	93.22±0.25	96.66±0.15	69.54±0.35

Table 9: Performance comparison in terms of model utility in the feature unlearning task.

Backbone	Method	PubMed	CiteSeer	Cora	CS	Physics	ogbn-arxiv
GCN	Retrain	42.82s	15.64s	8.31s	357.49s	1057.06s	173.59s
	BEKM	76.60s	12.92s	10.92s	66.88s	138.76s	1314.22s
	BLPA	65.70s	13.16s	11.36s	69.25s	140.64s	1424.94s
	GIF	0.40s	0.22s	0.21s	1.30s	1.92s	6.87s
	SR	30.81s	8.71s	8.80s	52.74s	149.74s	OOM
	Fast	30.71s	8.65s	8.71s	52.15s	152.54s	OOM
	MEGU	<u>0.30s</u>	<u>0.20s</u>	<u>0.19s</u>	<u>0.53s</u>	<u>1.04s</u>	<u>2.77s</u>
	ETR	0.01s	0.01s	0.01s	0.03s	0.05s	0.06s
GAT	Retrain	54.58s	18.28s	9.96s	369.58s	1079.54s	238.50s
	BEKM	112.55s	20.24s	17.11s	94.77s	182.37s	1435.04s
	BLPA	96.90s	20.47s	17.72s	97.58s	188.74s	1558.15s
	GIF	1.11s	0.68s	0.64s	2.10s	5.10s	11.56s
	SR	35.80s	12.97s	12.53s	56.25s	158.29s	OOM
	Fast	35.54s	12.22s	12.24s	58.30s	157.83s	OOM
	MEGU	<u>0.37s</u>	<u>0.23s</u>	<u>0.22s</u>	<u>0.66s</u>	<u>1.36s</u>	<u>3.64s</u>
	ETR	0.02s	0.02s	0.02s	0.04s	0.06s	0.08s

Table 10: Performance comparison in terms of unlearning efficiency in the edge unlearning task.

Backbone	Method	PubMed	CiteSeer	Cora	CS	Physics	ogbn-arxiv
GCN	Retrain	42.22s	15.60s	7.88s	322.21s	943.82s	168.91s
	BEKM	71.08s	12.95s	11.52s	71.71s	142.22s	1327.08s
	BLPA	68.97s	13.67s	11.63s	69.52s	143.42s	1320.60s
	GIF	0.39s	0.22s	<u>0.18s</u>	1.30s	1.94s	6.88s
	SR	30.34s	8.44s	8.73s	52.22s	148.24s	OOM
	Fast	30.92s	8.62s	8.35s	52.06s	147.64s	OOM
	MEGU	<u>0.31s</u>	<u>0.20s</u>	0.19s	<u>0.53s</u>	<u>1.05s</u>	<u>2.77s</u>
	ETR	0.01s	0.01s	0.01s	0.03s	0.05s	0.06s
GAT	Retrain	53.17s	17.84s	9.57s	332.11s	963.44s	235.38s
	BEKM	105.58s	20.42s	18.14s	100.69s	198.04s	1610.27s
	BLPA	101.28s	21.49s	19.09s	108.43s	231.09s	1595.64s
	GIF	1.12s	0.65s	0.59s	2.10s	5.09s	11.58s
	SR	36.00s	12.73s	12.12s	57.75s	169.89s	OOM
	Fast	35.85s	12.25s	12.08s	55.81s	159.12s	OOM
	MEGU	<u>0.37s</u>	<u>0.24s</u>	<u>0.22s</u>	<u>0.66s</u>	<u>1.37s</u>	<u>3.67s</u>
	ETR	0.02s	0.02s	0.02s	0.03s	0.06s	0.08s

Table 11: Performance comparison in terms of unlearning efficiency in the feature unlearning task.

Backbone	Method	PubMed	CiteSeer	Cora	CS	Physics	ogbn-arxiv
GCN	BEKM	0.095	0.10	0.0098	0.43	0.049	1.48
	BLPA	0.13	0.095	0.0088	0.43	0.050	1.53
	GIF	0.072	0.0045	0.029	0.029	0.22	1.44
	SR	0.085	0.051	0.016	0.0088	0.0019	OOM
	Fast	0.083	0.050	0.016	0.0088	0.0019	OOM
	MEGU	0.0085	<u>0.0023</u>	<u>0.0033</u>	<u>0.0012</u>	<u>0.00059</u>	<u>0.041</u>
	ETR	<u>0.015</u>	0.00015	0.00021	0.00026	0.00011	0.013
GAT	BEKM	0.010	0.015	0.030	0.015	0.0065	0.12
	BLPA	<u>0.011</u>	0.015	0.031	0.015	0.005	0.12
	GIF	0.10	0.0069	0.014	<u>0.0017</u>	0.0079	1.86
	SR	0.036	0.012	0.011	0.031	0.086	OOM
	Fast	0.034	0.014	0.011	0.031	0.086	OOM
	MEGU	0.082	<u>0.0012</u>	<u>0.0023</u>	0.023	<u>0.0022</u>	0.0033
	ETR	<u>0.011</u>	0.00040	0.00041	0.00029	0.00014	<u>0.016</u>

Table 12: Performance comparison in terms of unlearning efficacy in the edge unlearning task.

Backbone	Method	PubMed	CiteSeer	Cora	CS	Physics	ogbn-arxiv
GCN	BEKM	0.091	0.018	0.0092	0.035	0.055	1.43
	BLPA	0.097	0.014	0.0092	0.036	0.059	1.52
	GIF	0.072	0.0045	0.024	0.0098	0.035	1.55
	SR	0.082	0.0080	<u>0.0090</u>	0.0087	0.0023	OOM
	Fast	0.081	0.0079	<u>0.0093</u>	0.0088	0.0023	OOM
	MEGU	0.0084	<u>0.0024</u>	0.019	<u>0.00035</u>	<u>0.00058</u>	<u>0.041</u>
	ETR	<u>0.0090</u>	0.00011	0.00011	0.00023	0.00010	0.013
GAT	BEKM	<u>0.011</u>	0.014	0.051	0.0051	0.0084	0.65
	BLPA	<u>0.011</u>	0.013	0.055	0.0051	<u>0.0069</u>	0.66
	GIF	0.10	0.0070	0.040	0.033	0.0089	1.79
	SR	0.024	0.0036	0.0073	<u>0.0042</u>	0.097	OOM
	Fast	0.025	0.0036	0.0072	0.0043	0.097	OOM
	MEGU	0.081	<u>0.0012</u>	<u>0.0023</u>	0.023	0.012	0.0032
	ETR	0.0061	0.00029	0.00023	0.00028	0.00014	<u>0.012</u>

Table 13: Performance comparison in terms of unlearning efficacy in the feature unlearning task.